Langmuir
Article
pubs.acs.org/Langmuir

Substituent Effects on the Assembly of Helical Cyanine Dye Aggregates in the Minor Groove of a DNA Template†

Andrea L. Stadler,‡ Babu Rao Renikuntla, David Yaron, Adam S. Fang, and Bruce A. Armitage*

Department of Chemistry and Center for Nucleic Acids Science and Technology, Carnegie Mellon University, 4400 Fifth Avenue, Pittsburgh, Pennsylvania 15213-3890, United States. ‡ Current address: Biology Department, Brookhaven National Laboratory, Upton, New York 11973, United States.

Received October 28, 2010. Revised Manuscript Received November 24, 2010

Double-helical DNA was used as a template for the assembly of helical cyanine dye aggregates. The aggregates consist of cofacial dimers aligned end-to-end in the minor groove of the DNA. The effect of methoxy or fluoro substituents placed on the periphery of the cyanine dye heterocycles on aggregation both in water and on the DNA template was studied by UV−vis and circular dichroism spectroscopy. Methoxy groups were found to be stronger promoters of aggregation than fluoro, and a dimethoxy dye exhibited a higher propensity to aggregate compared with an unsymmetrical methoxy/fluoro dye. Semiempirical calculations supported the experimental observation of methoxy substitution favoring aggregation. These results indicate that dispersion and hydrophobic effects contribute more to dimerization/aggregation than do electron donor−acceptor effects.

Introduction

The use of covalent chemistry to synthesize precursor molecules that then self-assemble into larger, functional nanostructures is increasingly applied in the fields of nanoscience and nanotechnology. Although the information needed to specify the final supramolecular nanostructure can be encoded in the individual molecular components, a commonly used alternative is to rely on a template that can provide an underlying 1-D, 2-D, or 3-D scaffold on which to assemble the desired molecules. The scaffold can be removed later, if needed, or simply retained as part of the final nanostructure.

The versatility and efficiency of the design and synthesis of templated nanostructures by DNA is unparalleled in natural and artificial systems.[1] A high-level understanding of the directionality and stability of complementary base pairing allows the design of linear, branched, and higher-order (i.e., 3-D) assemblies having predictable sizes and structures. The use of computer-assisted-design software has pushed DNA nanotechnology into ever-more sophisticated and thought-provoking structures.[2−4]

Linear and multidimensional DNA nanostructures have been widely used as templating scaffolds to assemble other molecular components into supramolecular arrays.[1] Fluorescent dyes,[5] inorganic nanoparticles,[6,7] and proteins[8,9] have all been assembled in a controlled fashion using DNA templates.

In previous reports from our laboratory, we have shown that small organic dye molecules can assemble on DNA templates either by intercalation between base pairs[5] or by insertion into the minor groove.[10,11] The resulting aggregates can exhibit interesting optical properties, such as strong red- or blue-shifted absorption spectra, efficient energy migration and/or transfer pathways, and induced chirality (transferred from the helical DNA template to achiral dyes). In this report, we focus on dyes that assemble as helical aggregates within the minor groove of the DNA template. Our past work on these systems focused on varying the core structure of the dyes, namely, the specific heterocycles and conjugated bridge length.[12] We now describe the effects of peripheral substituents on the dyes, which can influence both the cofacial stacking of the dyes as well as the end-to-end alignment of dye dimers within the DNA groove.

Experimental Section

Materials. **H2** (**DiSC$_2$(5)**) was purchased from Molecular Probes (Eugene, OR) and used without further purification. Reagents for the synthesis of **F2**, **M2**, and **FM** were purchased from Sigma-Aldrich and Alfa-Aesar (USA). Solvents were HPLC grade. Stock solutions were prepared in methanol, and concentrations were determined spectrophotometrically in methanol using the following extinction coefficients: ε_{651} = 260 000 $M^{-1}cm^{-1}$ for **H2** (manufacturer's extinction coefficient), ε_{656} = 219 800 $M^{-1}cm^{-1}$ for **F2**, ε_{668} = 195 800 M^{-1} cm^{-1} for **M2**, and ε_{661} = 208 600 $M^{-1}cm^{-1}$ for **FM**. Synthetic procedures and the characterization of dyes are provided in the Supporting Information. [Poly(dI-dC)]$_2$ was purchased from GE Healthcare (Piscataway, NJ) and used as received. Stock solutions were prepared in aqueous sodium phosphate buffer (10 mM, pH 7.0), and concentrations were determined using ε_{251} = 13 800 M^{-1} cm^{-1} per base pair.

Equipment. ^{1}H NMR spectra were run on a Bruker Avance 300 MHz NMR spectrometer. ESI-MS spectra were taken on a Finnigan ESI/APCI ion trap mass spectrometer in positive mode.

† Part of the Supramolecular Chemistry at Interfaces special issue.

*Corresponding author. Tel: 412-268-4196. Fax: 412-268-1061. E-mail: army@cmu.edu.

(1) Becerril, H. A.; Woolley, A. T. *Chem. Soc. Rev.* **2009**, *38*, 329–337.
(2) Rothemund, P. W. K. *Nature* **2006**, *440*, 297–302.
(3) Andersen, E. S.; Dong, M.; Nielsen, M. M.; Jahn, K.; Lind-Thomsen, A.; Mamdouh, W.; Gothelf, K. V.; Besenbacher, F.; Kjems, J. *ACS Nano* **2008**, *6*, 1213–1218.
(4) Shih, W. M.; Lin, C. *Curr. Opin. Struct. Biol.* **2010**, *20*, 276–282.
(5) Benvin, A. L.; Creeger, Y.; Fisher, G. W.; Ballou, B.; Waggoner, A. S.; Armitage, B. A. *J. Am. Chem. Soc.* **2007**, *129*, 2025–2034.
(6) Alivisatos, A. P.; Johnsson, K. P.; Peng, X.; Wilson, T. E.; Loweth, C. J.; Bruchez, M. P. J.; Schultz, P. G. *Nature* **1996**, *382*, 609–611.
(7) Feldkamp, U.; Niemeyer, C. M. *Angew. Chem., Int. Ed.* **2006**, *45*, 1856–1876.
(8) Chhabra, R.; Sharma, J.; Ke, Y.; Liu, Y.; Rinker, S.; Lindsay, S.; Yan, H. *J. Am. Chem. Soc.* **2007**, *129*, 10304–10305.
(9) Kuzyk, A.; Laitinen, K. T.; Törmä, P. *Nanotechnology* **2009**, *20*, 235305/1–235305/5.
(10) Seifert, J. L.; Connor, R. E.; Kushon, S. A.; Wang, M.; Armitage, B. A. *J. Am. Chem. Soc.* **1999**, *121*, 2987–2995.
(11) Hannah, K. C.; Armitage, B. A. *Acc. Chem. Res.* **2004**, *37*, 845–853.
(12) Garoff, R.; Litzinger, E. A.; Connor, R. E.; Fishman, I.; Armitage, B. A. *Langmuir* **2002**, *18*, 6330–6337.

Chart 1

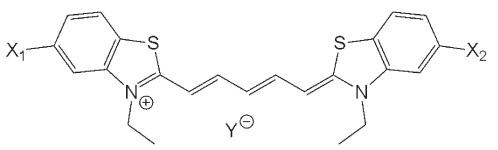

H2: $X_1 = X_2 = H$, Y = I

F2: $X_1 = X_2 = F$, $Y = CF_3CO_2$

M2: $X_1 = X_2 = OCH_3$, $Y = CF_3CO_2$

FM: $X_1 = F$, $X_2 = OCH_3$, $Y = CF_3CO_2$

UV−vis measurements were performed on a Varian Cary3 Bio spectrophotometer. Circular dichroism spectra were recorded on a Jasco J-715 instrument. The temperature was set to 20 °C on both instruments using thermoelectrically controlled cell holders.

UV−Vis Titrations. Dye solutions (2.0 μM each) were prepared in 10 mM sodium phosphate (pH 7.0) and 20% methanol. Titrations were performed by adding 0.5 μM aliquots of the annealed DNA duplex to the respective dye solutions. Samples were equilibrated at 20 °C for 5 min prior to scanning.

Temperature-Dependent Spectroscopy. In temperature-dependent UV−vis spectra, samples containing 2.0 μM dye and 5.0 μM DNA base pairs in 10 mM sodium phosphate buffer (pH 7.0) and 20% methanol were heated to 40 °C and equilibrated for 5 min prior to acquiring spectra. Subsequent spectra were recorded in 5 °C intervals down to 10 °C. At each data point, samples were equilibrated for 5 min prior to scanning. To determine the fraction dimerized on the DNA template, we first measured the absorbance at the monomer (A_M) and dimer (A_D) wavelengths for each dye and calculated the ratio A_D/A_M. We then calculated the same ratio for the dyes in methanol, where the dyes are in the monomeric state. For the four dyes, the A_D/A_M ratio in methanol varied only slightly in the range of 0.21−0.25. Assuming that the corresponding ratio for the DNA-templated dimers would also vary only slightly, we can estimate the fraction dimerized by the equation

$$\text{fraction dimerized} = \frac{(A_D/A_M)^T - (A_D/A_M)^{MeOH}}{9.92 - (A_D/A_M)^{MeOH}}$$

where $(A_D/A_M)^T$ and $(A_D/A_M)^{MeOH}$ correspond to the absorbance ratios at a given temperature T in Figure 9 and in methanol, respectively. The value of 9.92 comes from assuming that dye **M2** is completely dimerized on DNA at the lowest temperature and that the value will be similar for the other dyes. Thus, the values plotted in Figure 10 are estimates, but they should be reasonably close to the actual values that would be obtained if complete dimerization could be observed for each of the dyes.

CD Spectropolarimetry. CD spectra were acquired over the relevant wavelength range using a scan rate of 100 nm/min. A total of six scans were averaged to produce the spectra shown in the text. CD-temperature-dependent studies were performed as described for UV−vis.

Determination of Dimerization Equilibrium Constants. Equilibrium constants for dimerization (K) in homogeneous solution were calculated using the method of West and Pearce.[13] First, ε of the monomeric dye was assumed to be the same as in methanol, allowing the concentration determination of the monomeric dye (C_M) at the λ_{max} of the monomer absorbance peak. The dimeric dye concentration (C_D) was calculated using eq 1, and then K was calculated with eq 2:

$$C_D = \frac{C - C_M}{2} \quad (1)$$

$$K_d = \frac{C_D}{C_M^2} \quad (2)$$

(13) West, W.; Pearce, S. *J. Phys. Chem.* **1965**, *69*, 1894–1903.

Calculations. Semiempirical quantum chemistry was used to explore the interaction energy as a function of the relative orientation of the dyes. The structure of the isolated dyes was first optimized using the AM1 model,[14,15] with constraints applied to keep the conjugated core (all heavy atoms in the heterocycles and the bridge) planar. Dimer geometries were then obtained by displacing one of the dyes by R_{sep} perpendicular to the molecular plane and R_{shift} along the long axis of the molecule (where the long axis is defined as the principle inertial axis with the smallest moment of inertia). The conjugated core of both dyes was then held fixed while the positions of all attached groups, other than hydrogen atoms, were optimized. The interaction energies were obtained as the difference between the energy of the isolated dyes and the energy of the dimer.

The Coulomb interactions between dyes were obtained as a sum of interactions between atomic charges. The atomic charges are Mulliken charges from AM1 calculations on the isolated dyes, with charges on the hydrogen atoms summed into the heavy atoms. The Coulomb interaction is then obtained by using these charges with the optimized dimer geometries obtained above.

Results

Design. DNA-templated cyanine dye aggregates assemble in the minor groove of alternating deoxyadenosine-thymidine or deoxyinosine-deoxycytidine sequences.[11] The assembly of these helical aggregates was first described for dicarbocyanine dye **H2** (Chart 1, referred to as $DiSC_2(5)$ in our previous publications), with the initial formation of a face-to-face H dimer followed by end-to-end propagation of the aggregate, filling the length of the minor groove.[10] Dimerization within the minor groove of specific DNA sequences has been reported for other natural and synthetic compounds, particularly oligo-heterocycles such as distamycin[16] and analogues.[17]

Most of our prior work relied on cyanine dyes that have only hydrogen atoms on the periphery of the aromatic rings, although one example of a polyfluorinated dye was synthesized and found to have significantly reduced aggregation.[18] We have subsequently synthesized variations of **H2** in which the C-5 hydrogens on the peripheral benzothiazole groups were replaced by either fluoro (**F2**) or methoxy (**M2**) substituents. In addition, an unsymmetrical version with both fluoro and methoxy substituents (**FM**) was synthesized.

The substituents on these dyes were expected to influence aggregation for several reasons. First, by altering the water solubility of the dye, the substituents could influence the equilibria for both DNA binding and dimerization. Second, the substituents could impose steric constraints on both the face-to-face and end-to-end assembly of the aggregates in the DNA minor groove. Third, the substituents alter the electron distribution in the dyes. In addition to changing the partial charges on the benzothiazole

(14) Dewar, M. J. S.; Zoebisch, E. G.; Healy, E. F.; Stewart, J. J. P. *J. Am. Chem. Soc.* **1985**, *107*, 3902–3909.
(15) *AMPAC*, version 8; Semichem, Inc.: Shawnee, KS; 1992−1994.
(16) Pelton, J. G.; Wemmer, D. E. *Proc. Natl. Acad. Sci. U.S.A.* **1989**, *86*, 5723–5727.
(17) Dervan, P. B.; Edelson, B. S. *Curr. Opin. Struct. Biol.* **2003**, *13*, 284–299.
(18) Renikuntla, B. R.; Rose, H. C.; Eldo, J.; Waggoner, A. S.; Armitage, B. A. *Org. Lett.* **2004**, *6*, 909–912.

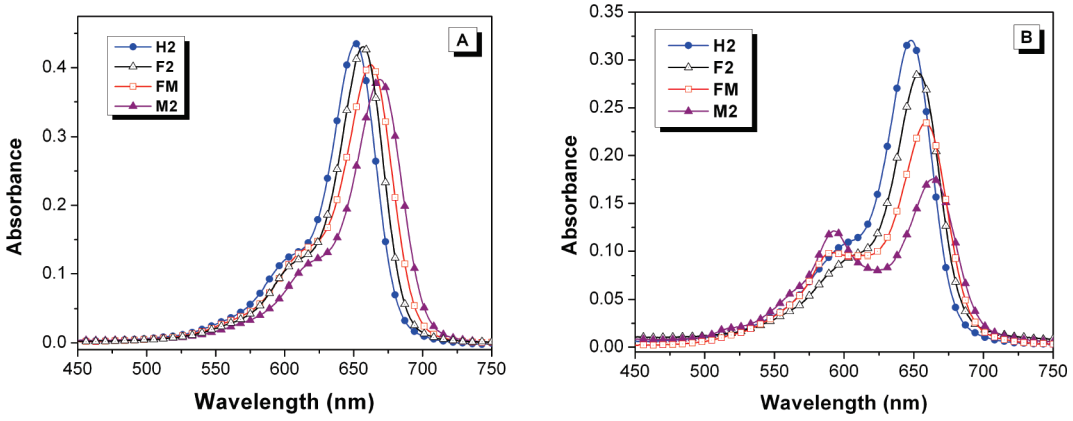

Figure 1. UV−vis absorption spectra for 2 μM solutions of dye in 100% methanol (A) and 20% MeOH, 10 mM sodium phosphate buffer (pH 7.0) (B).

rings, the substituents can affect the delocalization of the positive charge on the dye. This charge is delocalized equally between the two nitrogens in symmetric molecules **H2**, **F2**, and **M2** whereas the design of **FM** should lead to charge localization. Specifically, the electron-donating methoxy group of **FM** should stabilize a positive charge on that side of the molecule, and the withdrawing character of the fluoro substituent should have the opposite effect. The polarization of **FM** imparted by the incorporation of complementary donor/acceptor features on a single dye could enhance the π stacking of the dyes by encouraging an antiparallel orientation in which the Coulombic repulsions are minimized compared to those of symmetric dyes **H2**, **F2**, and **M2**.

Spectroscopic Characterization in Solution. Cyanine dye **H2** was previously shown to bind in the minor groove of DNA as an extended aggregate of H dimers. Prior to investigating the DNA binding properties of the dyes, we studied their behavior at low concentrations in methanol, water, and aqueous buffer. In methanol, the dyes are dissolved in the monomeric state and exhibit similar absorption spectra (Figure 1). Compared to **H2**, both electron-donating and electron-withdrawing substituents result in a bathochromic shift in the absorption spectrum and lower extinction coefficients. Polyfluorination was previously reported to have this effect on a symmetrical cyanine dye.[18]

Many types of dyes are known to aggregate in aqueous solution, leading to a lower intensity of the monomer band and the emergence of additional bands at other wavelengths.[13,19] These spectral changes are attributed to the face-to-face assembly of the dye molecules into dimers and higher-order aggregates, stabilized by π-stacking interactions and the hydrophobic effect. In aqueous buffer, the spectra of **H2** and **F2** closely resemble their respective spectra in methanol (Figure 1). However, differences appear in the spectra when the methoxy substituent is present. Dye aggregation is revealed by the appearance of a hypsochromically shifted peak for **M2** and, to a lesser extent, **FM**. The propensity of **M2** to aggregate was demonstrated by an almost 50% loss of monomer absorption in aqueous buffer. The fact that the symmetrical dye aggregates more than the unsymmetrical dye indicates that aggregation is driven more by hydrophobicity than by complementary electrostatic interactions.

We sought to determine quantitatively the propensity of the substituted dyes to aggregate in the absence of a template. Using the method developed by West and Pearce,[13] we determined the dissociation constant of the dimer in pure water for **H2** to be $K_d = 1.9 \times 10^{-5}$ M^{-1}, which compares favorably to the literature

Scheme 1

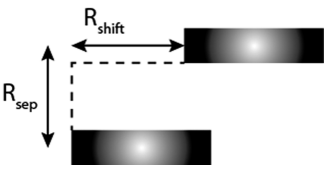

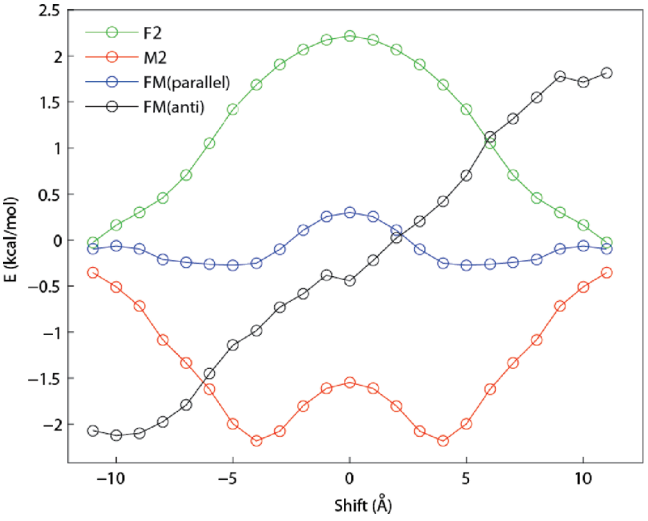

Figure 2. Dimerization energies of substituted cyanine dyes, relative to that of the unsubstituted dye, as a function of R_{shift} with R_{sep} = 4 Å.

value ($K_d = 1.5 \times 10^{-5}$ M^{-1}).[13] Meanwhile, the dimerization of difluoro analogue **F2** is 3 times more favorable than that of parent dye **H2** ($K_d = 6.3 \times 10^{-6}$ M^{-1}). Dilute solutions of dyes bearing methoxy substituents readily form higher-order aggregates in pure water (Supporting Information, Figure S1), preventing the determination of the dimerization constant for **M2** and **FM**.

Modeling of Dye Aggregates. The semiempirical quantum chemical approach described in the Experimental Section was used to model the interactions between the cyanine dyes, with the goal of understanding the effects of the substituents on the interaction energies. The AM1 model was used to obtain the dimerization energy, defined as the difference between the energy of the dimer and the isolated dyes. Because of the strong Coulomb repulsion between these charged dyes, the interaction is strongly repulsive in the absence of solvent. We therefore focus on the

(19) Herz, A. H. *Photog. Sci. Eng.* **1974**, *18*, 323–335.

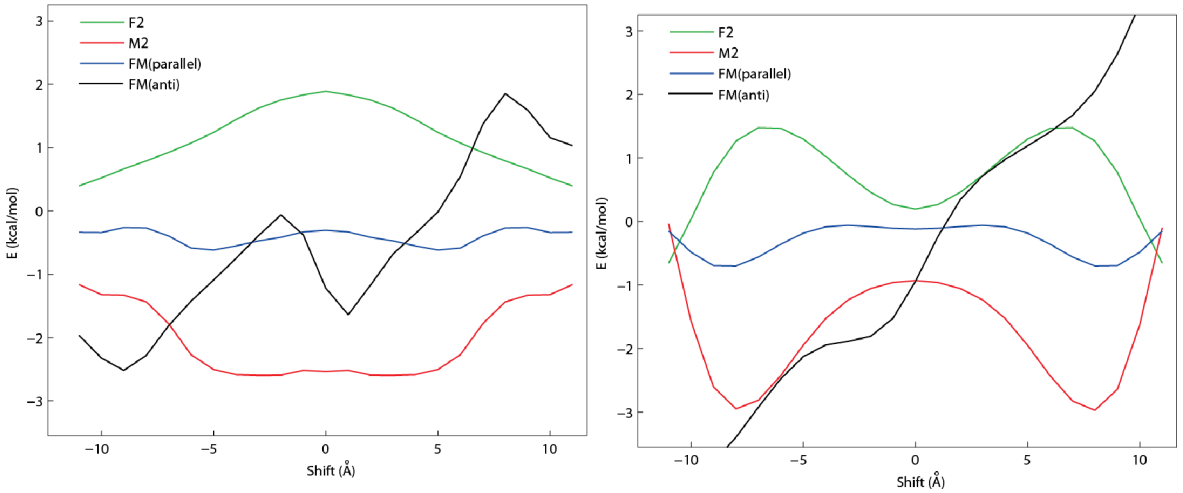

Figure 3. Dimerization energies of substituted cyanine dyes, relative to that of the unsubstituted dye, obtained from interactions between atomic charges (left panel) and interactions between the point charges of Figure 4 (right panel). The colors are the same as in Figure 2.

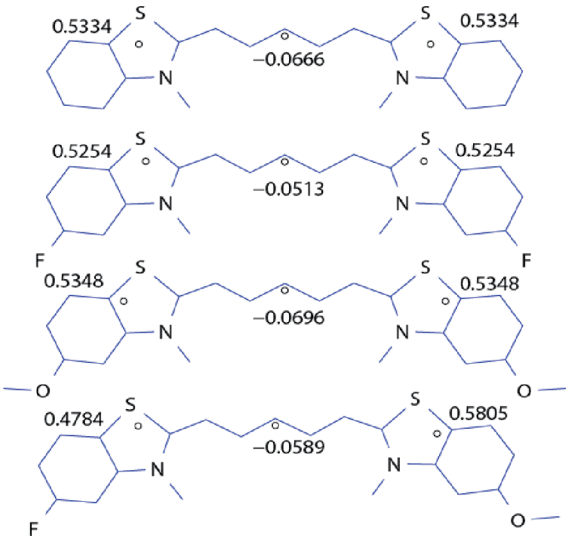

Figure 4. Group charge locations (circles) and magnitudes of the bridge and heterocycles of the dyes. These charges summarize the charge distributions of the dyes.

effects of the substituents on the interaction energy for various dimer geometries. The geometries correspond to planar dyes separated by a distance R_{sep} in a direction perpendicular to the molecular plane and shifted by R_{shift} along the long axis of the dye (Scheme 1). The substituent effect is defined as the difference between the dimerization energy of the substituted dyes and that of the unsubstituted dyes.

Figure 2 shows the effects of substituents on the dimerization energy as a function of R_{shift} for a fixed interplanar separation, R_{sep}, of 4 Å. (The same relative ordering of interaction energies is obtained for R_{sep} of 3.5 and 4.5 Å, which spans the range of expected separation between cyanines.[20]) The range of shifts shown in the Figure corresponds to the distance between the centers of the heterocycles such that at the extremes of the range two heterocycles are eclipsed and two are out of contact with the other dye. The results for symmetrically substituted dyes show that fluorine substituents destabilize the dimer and methoxy substituents stabilize the dimer. For the asymmetrically substituted dyes, the interaction energy lies between that of the symmetric dyes for shifts of less than about 6 Å and for both parallel and antiparallel arrangements. (The substituent effects of the asymmetric dye are more stabilizing than those of the symmetric dyes only when the shift is such that the fluorine-substituted heterocycles are eclipsed, whereas the methoxy substitutents are out of contact with the other dye.) This is counter to what may be expected for neutral dyes, such as the merocyanines studied by Würthner and colleagues, where the dipole induced by asymmetric substitution would substantially increase the interaction energy for the antiparallel arrangement, even for small shifts.[21]

To understand the origin of the trends seen in Figure 2, we first consider the degree to which the interaction may be understood in terms of interactions between atomic charges.[22] The left panel of Figure 3 shows that the interaction between atomic charges exhibits the same trends as seen for the AM1 calculations of Figure 2.

The simplest representation of the charge distribution we could find, which captures the relative order of the binding energies, is shown in Figure 4. The atoms of each dye were divided into three groups corresponding to the two heterocycles and the bridge. The atomic charges on each of these groups were then collapsed to a single point. For the heterocycles, this point is taken as the center of charge. For the bridge, the point is taken as the center of the bridge. The resulting charges and locations are shown in Figure 4. The charges can be rationalized in terms of F substituents pushing positive charge toward the bridge and methoxy substituents pulling positive charge away from the bridge. The right panel of Figure 3 shows the interaction energies between these three charges. The results show that, whereas this simplification introduces some substantial differences from the AM1 results, the trends are the same as for the full AM1 calculations. The charges in Figure 4 therefore capture the essential aspects of the interactions. Even though the asymmetrically substituted dye has an asymmetric charge distribution, the dimerization energy is intermediate between that of the corresponding symmetrically substituted dyes. Note that this behavior is quite distinct from what would be expected for uncharged dyes, where the dipole moment on the asymmetric dye would be expected to enhance the dimerization energy strongly.[21]

The above calculations are quite approximate, with the largest error likely coming from the absence of solvent in the model.

(20) Tomlinson, A.; Frezza, B.; Kofke, M.; Wang, M.; Armitage, B. A.; Yaron, D. *Chem. Phys.* **2006**, *325*, 36–47.

(21) Würthner, F.; Yao, S. *Angew. Chem., Int. Ed.* **2000**, *39*, 1978–1981.

(22) Wheeler, S. E.; Houk, K. N. *J. Am. Chem. Soc.* **2008**, *130*, 10854–10855.

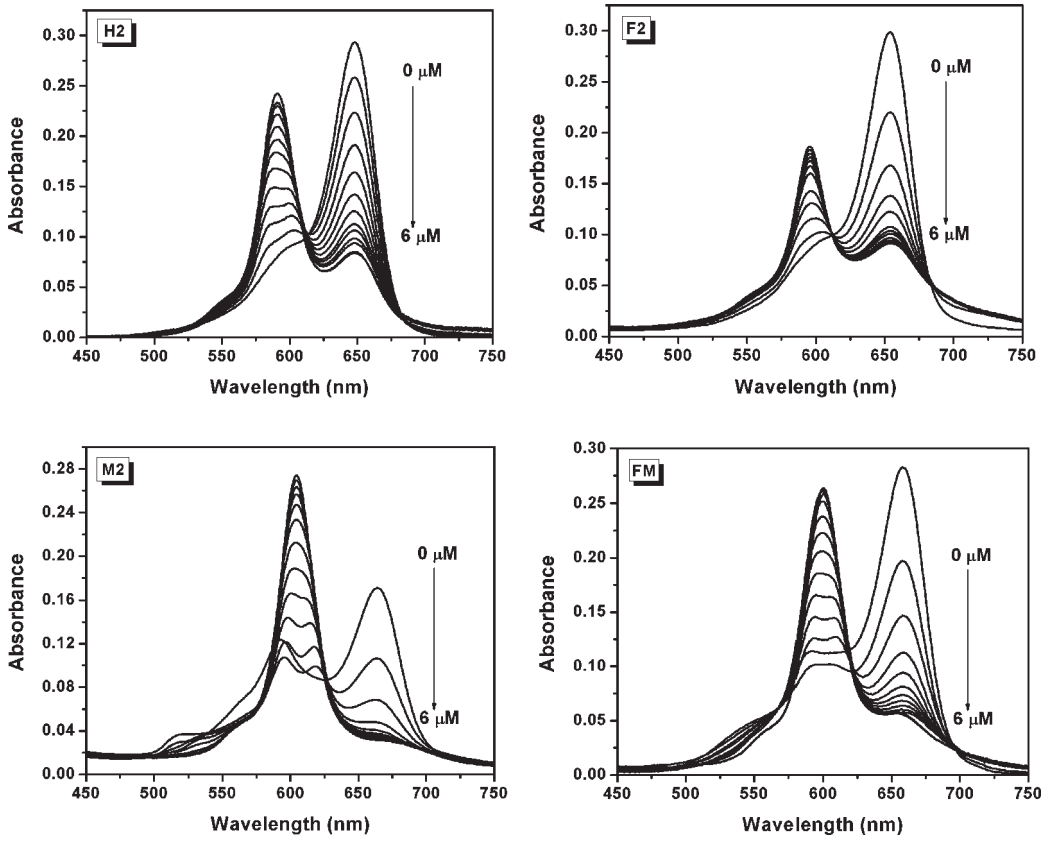

Figure 5. UV−vis analysis of the titration of $[poly(dI\text{-}dC)]_2$ into 2.0 μM solutions of cyanine dye in 10 mM sodium phosphate (pH 7.0) and 20% methanol. DNA was added in 0.5 μM aliquots. Data were recorded at 20 °C.

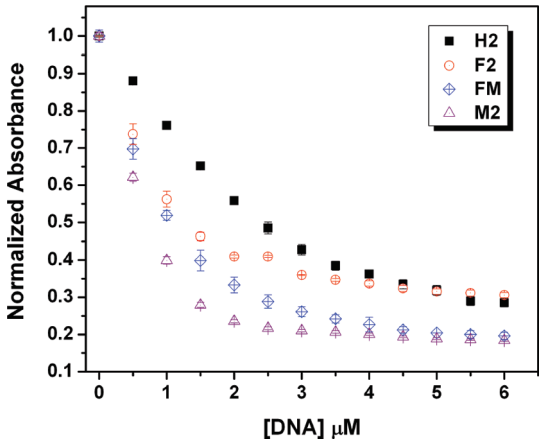

Figure 6. Comparison of the attenuation of dye monomer absorbance as the DNA concentration is increased. Data were taken from Figure 4 and normalized to [DNA] = 0.

Nevertheless, the results rationalize the experimental observation that **M2** aggregates more strongly than **F2**, with asymmetrically substituted dye **FM** having an intermediate interaction strength. The computations also indicate that **F2** should aggregate less strongly than the unsubstituted dye **H2**, although this is not observed experimentally. This disagreement may be due to hydrophobic effects arising from the fluorine substituents, which would drive aggregation and are not included in the above model.

DNA-Templated Aggregation. Using DNA template $[poly(dI\text{-}dC)]_2$, we varied both the concentration of DNA and the temperature of examining the aggregation propensity of the

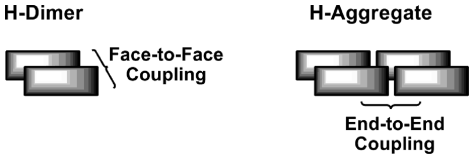

Figure 7. Electronic coupling in cyanine dye aggregates. The DNA template precludes growth beyond a dimer in the face-to-face direction, but adjacent dimers can exhibit end-to-end coupling.

substituted dyes. The titration of the DNA template into dye solutions in aqueous buffer results in a significant attenuation of the monomer band (Figures 5 and 6). For all of the dyes, as the concentration of DNA increases, the growth of a blue-shifted H-dimer/aggregate peak is observed. As was the case in water, DNA-templated aggregation is most efficient for methoxy-substituted dyes **M2** and **FM**. (The lack of isosbestic points for the titrations involving these dyes is attributed to the presence of monomer, dimer, and higher aggregate before DNA is even added to the cuvette.) These results indicate that the DNA acts as a template to promote well-ordered dimer formation for the new substituted dyes.

At low DNA/dye ratios, splitting of the H band is observed for **H2**, **M2**, and **FM**. This splitting is due to the end-to-end coupling of adjacent dimers. In the presence of a DNA template, orbital overlap between dye molecules occurs in both the face-to-face and end-to-end directions (Figure 7). As the DNA concentration increases, the splitting is lost because the dimers begin to spread out along the minor groove, reducing the strength of the end-to-end coupling. This effect will be more evident in circular dichroism spectra shown below.

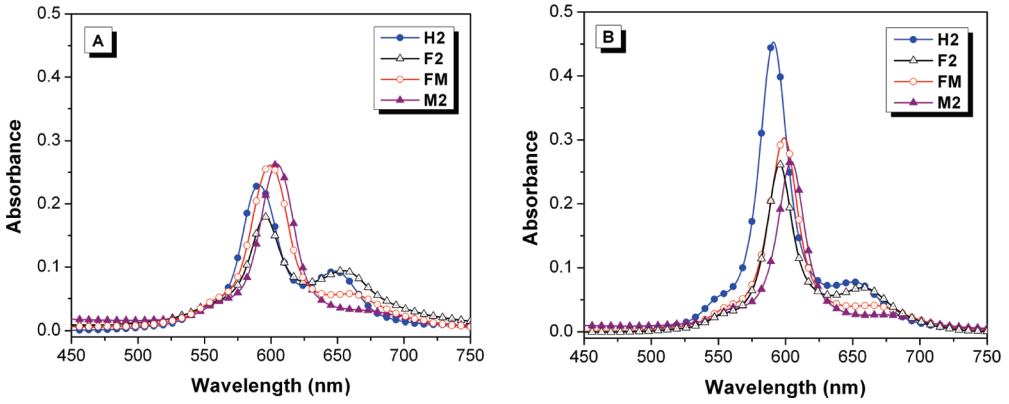

Figure 8. Effect of DNA concentration on cyanine dye aggregation. [DNA] = 5.0 μM base pairs (A) or 20 μM base pairs (B). [Dye] = 2.0 μM. Spectra were recorded at 20 °C.

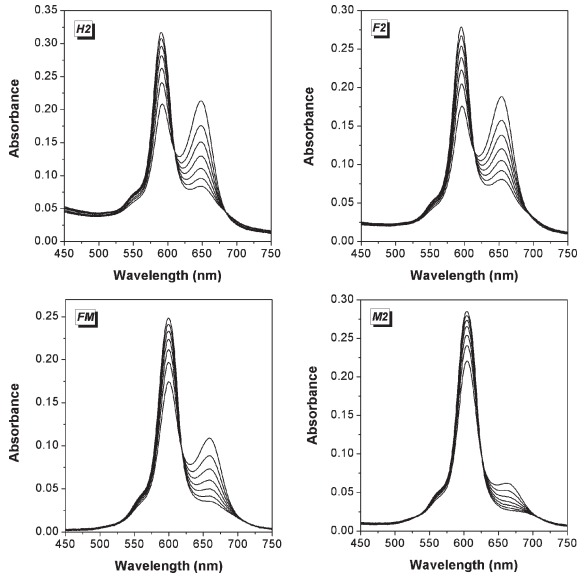

Figure 9. Temperature dependent UV−vis spectra of 2 μM dye with 5 μM [poly(dI-dC)]$_2$. Spectra were recorded at 5 °C intervals from 10 to 40 °C. The buffer contained 10 mM sodium phosphate buffer (pH 7) and 20% methanol.

The average length of the DNA template was 200 base pairs. On the basis of the length of the dyes, each dimer should cover approximately five or six base pairs, leading to the formation of extended helical aggregates that contain up to 40 dimers.[10] At a concentration of 5 μM base pairs, the DNA template should be saturated in the presence of 2 μM dye. UV−vis analysis shows that symmetric dye **M2** is primarily present in the dimeric state with almost no monomer evident in the spectrum (Figure 8A). Unsymmetrical dye **FM** exhibits some residual monomer absorption whereas there is substantially more monomer evident in the spectra for **H2** and **F2**. When the concentration of DNA is increased to 20 μM base pairs, the dimer peak nearly doubles in intensity for **H2** with smaller increases for **F2** and **FM** (Figure 8B). The spectrum narrows slightly for all of the dyes. The additional DNA binding sites evidently allow the dimers to spread out along the DNA template, thus reducing the repulsive Coulombic forces between dimers and enhancing dimerization.

We next investigated the thermal stability of the DNA-templated aggregates. Heating the samples from 10 to 40 °C destabilizes the aggregates, leading to the attenuation of the blue-shifted H-band accompanied by an enhancement of the monomer

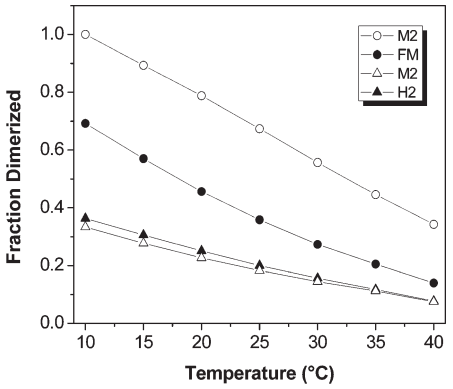

Figure 10. Plot of the fraction dimerized as a function of temperature based on the spectral data in Figure 9. The fraction dimerized was estimated as described in the Experimental Section.

peak (Figure 9). Temperatures greater than 40 °C were not investigated because the DNA template denatures into single strands, destroying the minor groove. **H2** and **F2** exhibit similar spectra over the entire temperature range, whereas **FM** and **M2** clearly form much more dimer at each temperature.

The ratio of the absorbances due to monomer and dimer is a measure of the aggregate stability, with a lower ratio corresponding to a more stable aggregate. As described in the Experimental Section, this ratio can be converted into an estimate of the fraction dimerized. As shown in Figure 10, the fraction dimerized for dimethoxy dye **M2** at the highest temperature (0.4) is comparable to the fraction dimerized for **H2** and **F2** at the lowest temperature.

The end-to-end coupling manifested as dimer peak broadening in the UV−vis titrations can be readily resolved using CD spectroscopy (Figure 11).[10] Binding of the achiral cyanine dyes to the chiral, right-handed DNA double helix induces chirality in the bound dimers. The overlap between adjacent dimers along the DNA template splits the excited state into an upper and lower transition, and a biphasic signal is observed to pass through zero at the maximum absorbance of the dimer. The relative position of the two peaks, where the positive peak is at a longer wavelength compared to the negative peak, is indicative of a right-handed relationship between dimers, which is expected on the basis of the right-handed helicity of the template.[23] The interdimer couplings can be calculated from the difference in energy between the positive and negative CD bands. The intra- and interdimer

(23) Nakanishi, K.; Berova, N.; Woody, R. W. *Circular Dichroism: Principles and Applications*; VCH Publishers: New York, 1994.

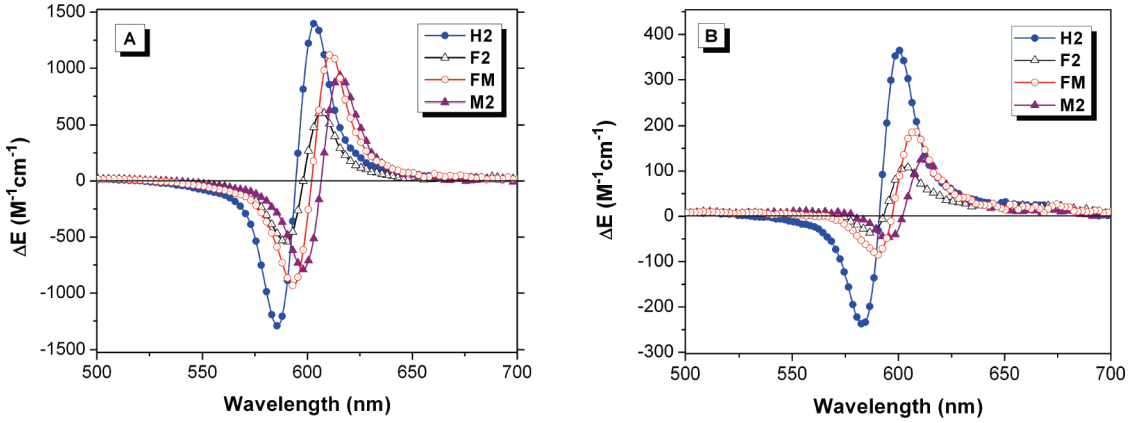

Figure 11. CD spectra of 2 μM dyes in the presence of 5 μM (right) and 20 μM (left) $[poly(dIdC)]_2$. Spectra were recorded at 20 °C and are the average of 10 scans collected at a scan rate of 200 nm/min.

Table 1. Intra- and Interdimer Electronic Couplings in DNA-Templated Dye Aggregates

dye	intradimer coupling (cm^{-1})[a]	interdimer coupling (cm^{-1})[b]
H2	3118	540
F2	3089	475
FM	3076	497
M2	3172	462

[a] Calculated as twice the difference in energy between the monomer and dimer UV−vis absorbance bands. [b] Calculated as the difference in energy between the positive and negative CD bands.

couplings obtained for the dyes when bound to $[poly(dI\text{-}dC)]_2$ are listed in Table 1. The splittings that arise from the face-to-face overlap are approximately 6-fold higher than the interdimer couplings that arise from end-to-end coupling, as observed previously for other DNA-templated cyanine dye aggregates.[12] The lower interdimer couplings for the substituted dyes relative to **H2** perhaps reflect steric and electrostatic repulsions that increase the distance between adjacent dimers within the groove of the DNA template.

The intensity of the CD signal is also indicative of the strength of interdimer coupling. Under saturation conditions (i.e., 1 dimer for 5 DNA base pairs), **H2** and **FM** exhibit CD signals with similar intensities (Figure 11A). The increased intensity of the CD signal for **M2** contrasted with that for **F2** indicates that **M2** dimers are closer together on the DNA template, in spite of the larger size of the methoxy group. When the DNA concentration is increased to 20 μM (i.e., 1 dimer for 20 DNA base pairs), the intensity of the induced CD signal decreases for all four dyes (Figure 11B). Under these conditions, the DNA template is no longer saturated, and the dimers can spread out along the template, leading to weaker interdimer couplings. This effect is more pronounced for the substituted dyes, where the substituents likely exert electrostatic and/or steric repulsions between dyes that approach each other in an end-to-end alignment.

Temperature-dependent CD studies are in agreement with the corresponding UV−vis analysis shown above (Supporting Information). As the temperature increased from 10 to 40 °C, the intensity of the CD signal decreased, corresponding to aggregate destabilization with the thermal stability following the order **M2** > **FM** > **F2** = **H2**.

Discussion

The results described above provide our first insight into the effects of peripheral substituents on cyanine dye aggregation in the minor groove of DNA. These substituents could influence dye

Chart 2

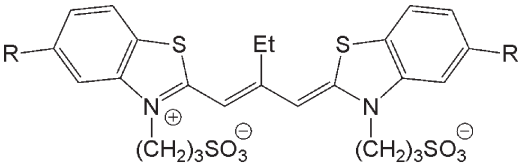

R = Cl, OCH_3

aggregation through steric, electronic (dipolar and/or dispersion), or hydrophobic factors. As is the case with unsubstituted dyes that differ in terms of the nature of the heterocycle (e.g., benzothiazole versus benzoxazole) or the methine bridge length (e.g., carbocyanine versus dicarbocyanine), our results indicate that dispersion and hydrophobic factors are dominant over dipolar effects because symmetrical dye **M2** aggregates more effectively than unsymmetrical dye **FM**, followed by **F2** and then **H2**. This order is observed both in aqueous buffer and in the minor groove of a double-helical DNA template. In terms of sterics, one might expect the opposite order because a methoxy group is clearly larger than a fluorine atom. Evidently even the relatively constrained environment of the DNA minor groove is able to accommodate the bulkier methoxy substituents without hindering the formation of face-to-face H dimers.

In relevant prior studies, Takahashi and co-workers reported aggregation studies for anionic carbocyanine dyes bearing chloro or methoxy groups at the 5 and 5′ positions of the benzothiazole units as shown in Chart 2.[24] The dimethoxy derivative formed H dimers analogous to the cationic dyes reported here with nearly a 4-fold-greater K_D than the chloro derivative. Because dye dimers and aggregates are stabilized by dispersion interactions, difluoro dye **F2** is expected to be even less likely to aggregate than a corresponding dichloro dye, although we have not synthesized other halo-substituted dyes.

We considered the possibility that unsymmetrical dye **FM** would exhibit the strongest dimerization because of dipolar interactions promoted by the donor and acceptor groups present on opposite ends of the molecule. Würthner and co-workers have exploited such dipolar interactions to drive the aggregation of uncharged merocyanine dyes in organic solvents such as dioxane,[21,25] but in the case of the charged cyanine dye core

(24) Takahashi, D.; Oda, H.; Izumi, T.; Hirohashi, R. *Dyes Pigments* **2005**, *66*, 1–6.
(25) Würthner, F.; Yao, S.; Debaerdemaeker, T.; Wortmann, R. *J. Am. Chem. Soc.* **2002**, *124*, 9431–9447.

studied here, the donor−acceptor effects are minimal. The insignificant electronic effects of the substituents are also reflected in the fact that the absorption maximum varies by only 18 nm and the most red-shifted spectrum belongs to **M2** rather than dipolar variant **FM**. Because aggregation, both in water and on the DNA template, correlates with the number of methoxy substituents on the dye, dispersion forces appear to be the dominant factor controlling the aggregation of these dyes.

Steric and electrostatic effects of the substituents have a much larger effect on the formation of extended dye aggregates in the DNA minor groove. In aqueous solution, aggregates propagate by adding additional monomers to the original dimer in a cofacial arrangement. The structural constraints of the minor groove limit aggregate growth in this direction to a dimer. However, extended aggregates can form by aligning individual dimers in an end-to-end arrangement. CD spectroscopy provides a sensitive technique for distinguishing electronic communication between adjacent dimers from interactions between the two monomers of an individual cofacial dimer. Whereas an isolated DNA-bound dimer gives a weak, positive CD band, the alignment of two dimers adjacent to one another in the minor groove gives rise to intense, split CD bands as a result of electronic coupling between the dimers, where chirality is induced through binding to the DNA template.

The CD spectra shown in Figure 11 provide insight into the effects of the substituents on the assembly of extended aggregates in the DNA groove. It is best to focus on the differential effects (i.e., comparing unsubstituted dye **H2** with the other dyes). In the first set of spectra (Figure 11A), the dyes are forced to form a compact aggregate because the dye to DNA ratio corresponds to 1 dimer for 5 base pairs. In Figure 11B, the dyes are allowed to spread out along the DNA by increasing the DNA concentration, giving a ratio of 1 dimer for 20 base pairs. The relative intensities of the CD spectra for the substituted dyes compared with **H2** decrease significantly, indicating that steric and/or electrostatic repulsions drive the substituted dimers further apart. Interestingly, **M2** loses the most intensity, indicating that the steric effect of the larger methoxy group is the most repulsive, compared with the smaller but presumably more electrostatically repulsive fluoro substituent.

Conclusions

These experiments indicate that DNA-templated cyanine dye aggregates are tolerant of peripheral substituents on the dye heterocycles. Although methoxy and fluoro groups enhance the dimerization of the dyes both in solution and in the DNA minor groove, the assembly of extended helical aggregates in DNA is suppressed by the substituents because of steric and electrostatic repulsive interactions introduced by the end-to-end alignment of dimers within the groove. To enhance both dimerization and helical aggregation, dyes with extended, unsubstituted heterocycles such as naphthothiazole are worthy of investigation.

Acknowledgment. This work was supported by a grant from the National Science Foundation (CHE 0315925 to B.A.A.). A.L.S. was supported by the Astrid and Bruce McWilliams Fellowship.

Supporting Information Available: Synthesis details for substituted cyanine dyes **M2**, **F2**, and **FM**. UV−vis spectra showing the aggregation of **M2** in water. Temperature-dependent CD spectra for DNA-templated dye aggregates. This material is available free of charge via the Internet at http://pubs.acs.org.